Evaluating Vascularization of Heterotopic Islet Constructs for Type 1 Diabetes Using an In Vitro Platform

Article *in* Integrative Biology · November 2019

DOI: 10.1093/intbio/zyz027

CITATIONS
5

READS
38

5 authors, including:

Annie Bowles
University of Miami Miller School of Medicine
76 PUBLICATIONS **1,022** CITATIONS
SEE PROFILE

Matthew Ishahak
University of Miami
14 PUBLICATIONS **174** CITATIONS
SEE PROFILE

Diego Correa
University of Miami Miller School of Medicine
84 PUBLICATIONS **4,048** CITATIONS
SEE PROFILE

Ashutosh Agarwal
Stanford University
40 PUBLICATIONS **569** CITATIONS
SEE PROFILE

OXFORD

Integrative Biology, 2019, 11(8),331–341

doi: 10.1093/intbio/zyz027
Advance Access publication November 13, 2019
Original Article

ORIGINAL ARTICLE

Evaluating Vascularization of Heterotopic Islet Constructs for Type 1 Diabetes Using an *In Vitro* Platform

Annie C. Bowles[1,2,3,4], Matthew M. Ishahak[1,2], Samuel J. Glover[1], Diego Correa[2,3,4], and Ashutosh Agarwal[1,2,3,*]

[1]Department of Biomedical Engineering, University of Miami, Coral Gables, FL, USA, [2]DJTMF Biomedical Nanotechnology Institute at the University of Miami, Miami, FL, USA, [3]Diabetes Research Institute, Miller School of Medicine, University of Miami, Miami, FL, USA, and [4]Department of Orthopaedics, UHealth Sports Medicine Institute, University of Miami, Miami, FL, USA

***Corresponding author:** E-mail: a.agarwal2@miami.edu

Abstract

Type 1 diabetes (T1D) results from the autoimmune destruction of β-cells within the pancreatic islets of Langerhans. Clinical islet transplantation from healthy donors is proposed to ameliorate symptoms, improve quality of life, and enhance the life span of afflicted T1D patients. However, post-transplant outcomes are dependent on the survival of the transplanted islets, which relies on the engraftment of the islets with the recipient's vasculature among other factors. Treatment strategies to improve engraftment include combining islets with supporting cells including endothelial cells (EC) and mesenchymal stem cells (MSC), dynamic cells capable of robust immunomodulatory and vasculogenic effects. In this study, we developed an *in vitro* model of transplantation to investigate the cellular mechanisms that enhance rapid vascularization of heterotopic islet constructs. Self-assembled vascular beds of fluorescently stained EC served as reproducible *in vitro* transplantation sites. Heterotopic islet constructs composed of islets, EC, and MSC were transferred to vascular beds for modeling transplantation. Time-lapsed imaging was performed for analysis of the vascular bed remodeling for parameters of neo-vascularization. Moreover, sampling of media following modeled transplantation showed secretory profiles that were correlated with imaging analyses as well as with islet function using glucose-stimulated insulin secretion. Together, evidence revealed that heterotopic constructs consisting of islets, EC, and MSC exhibited the most rapid recruitment and robust branching of cells from the vascular beds suggesting enhanced neo-vascularization compared to islets alone and control constructs. Together, this evidence supports a promising cell transplantation strategy for T1D and also demonstrates a valuable tool for rapidly investigating candidate cellular therapies for transplantation.

Keywords: cell transplantation; type 1 diabetes; pancreatic islets; mesenchymal stem cells

Received May 13, 2019; **revised** September 3, 2019; **editorial decision** September 4, 2019; **accepted** September 4, 2019

INSIGHT

Type 1 diabetes results from autoimmune destruction of insulin-producing cells within the pancreatic islets of Langerhans. Cellular therapy approaches have the potential to restore the function. However, standard transplantation of cadaveric islets is especially limited by inadequate engraftment of transplanted islets with the host vasculature and incitement of a robust immune response. Strategies to improve outcomes have been focused on developing heterotypic islet constructs that combine islets with endothelial and mesenchymal stem cells. We present an *in vitro* platform to rapidly evaluate the efficacy of these heterotopic constructs to engraft with the host vasculature. Our platform allows visualization and quantification of such events, along with collection of secretome, and is ideally suited for evaluating candidate cellular therapies prior to transplantation.

INTRODUCTION

Type 1 diabetes (T1D) is an autoimmune disease that leads to the destruction of the functional unit of the pancreas called the islets of Langerhans. Islets are multicellular clusters closely associated with the vasculature making its critical endocrine function, i.e. secreting hormones like insulin in response to molecular signals in the blood, a vital role for maintaining cell metabolism and proper function of all body systems [1, 2]. Currently, there is no cure for T1D, and patients are unable to maintain blood glucose levels without exogenous insulin, supplements, and dietary regulation, all of which are unable to prevent long-term complications and improve quality of life [3–5].

Large efforts to achieve clinical success with islet transplantation have been explored as a plausible solution for patients with T1D. However, preclinical and clinical studies of pancreatic islet transplantation for T1D have elucidated some limitations surrounding vascularization and engraftment of islet transplants, and in turn, the cells' survival and clinical outcomes [6–8]. The close proximity of islets to the vasculature, thus oxygen-rich requirements, results in the added difficulty of transplant survival directly after transplantation. Efforts to improve engraftment of pancreatic islets include co-transplantation strategies with the addition of mesenchymal stem cells (MSC) [9, 10], which are robust cells with known vascular-mediating propensities, and endothelial cells (EC) [11, 12], the cellular building blocks of the vasculature. Strategies for organoid constructs have often combined both MSC and EC with organ-specific cells and tissues to re-create the integral components to an organ system [10, 13]. Moreover, the cultured heterotopic islet constructs containing EC and MSC have demonstrated marked success with initiating intravascular network assembly prior to transplantation that has shown to greatly improve engraftment after transplantation in preclinical studies [10].

Here, we describe an *in vitro* platform that models neo-vascularization of heterotopic islet constructs in parallel with control groups to access the mechanistic activities correlative to each type of islet construct to better understand ways to potentially improve islet cell therapy. Vascular beds composed of endothelial cell (vb-EC) networks were assembled in the wells of 96-well plates as an easy and reproducible representation of transplantation sites. Simultaneously, human donor pancreatic islets were isolated and designated into four experimental groups: Group 1 (islets only, current standard), Group 2 (islets and EC), Group 3 (islets and MSC), and Group 4 (islets, EC, and MSC). Using these multicellular combinations provided insight into the contributions to vascularization potential for each construct. By fluorescence imaging, we were able to visualize the daily alterations of the construct with regards to the vascular bed networks. As early as 24 h, we were able to see a vb-EC remodeling proximal to the constructs prepared with MSC (i.e. Groups 3 and 4) and integration into the constructs by 72 h. This evidence was supported by quantitative parameters defined as neo-vascularization and branching associated with vb-EC and islet constructs. Moreover, sampling of the media generated profiles of key mediators, including the insulin-like growth factor (IGF) binding protein family, which were differentially modulated during the first 24 h of neo-vascularization. Following neo-vascularization measurements and sampling, we were capable of performing static glucose-stimulated insulin secretion (GSIS) functional assays on this platform. Together, Group 4 islets (islets, EC and MSC) outperformed all other groups by demonstrating the most rapid and robust recruitment of vb-EC to assimilate neo-vascularization in modeled transplantation (Model-Tx). Our results not only permit access into the rapidly changing processes that occur after 'transplantation', but further support the use of MSC as promoters for enhanced neo-vascularization. This methodology of Model-Tx also supports a valuable tool for modeling transplantation *in vitro* for candidate cell transplantation therapies.

MATERIALS AND METHODS

Cell culture, staining and formation of islet constructs

Human-bone-marrow-derived MSC were isolated from bone marrow aspirates obtained from de-identified healthy donors after provided written informed consent. All procedures were carried out in accordance with relevant guidelines and regulations, following a protocol approved by the Case Stem Cell Facility Institutional Review Board (IRB) (approval # 09-90-195). Cells were cultured as adherent cells in a humidified incubator set to 37°C and 5% CO_2 in complete culture media (CCM) containing Dulbecco's modified eagle medium (Gibco, Thermo Fisher Scientific, Waltham, MA) and 10% fetal bovine serum (Seradigm, VWR, Radnor, PA), which was replaced every 3–4 days. Upon reaching 80% confluency, cells were passaged at a 1: 10 ratio by detaching with TrypLE™ Select Enzyme ×1 (Gibco, Thermo Fisher Scientific) and counted by live/dead exclusion method using 0.4% trypan blue (Invitrogen, Carlsbad, CA). MSC were used at passage 3 for all experiments. Human umbilical vein EC (PromoCell, Heidelberg, Germany) were cultured as adherent cells in a humidified incubator set to 37°C and 5% CO_2 in complete endothelial growth media 2 (EGM-2; PromoCell),

which was replaced every 3 days. EC were used at passages 3–5 for all experiments.

Human pancreatic islets were procured from deceased organ donors at the Diabetes Research Institute Cell Processing cGMP Facility (University of Miami, Miller School of Medicine, Miami, FL). Institutional Review Board exemption was obtained for pancreatic islets used for research. Harvested islets were cultured in complete islet media containing Prodo islet Media (standard) with human AB serum supplement (5%), glutamine/glutathione supplement (2%), all purchased from PRODO Laboratories, Inc. (Irvine, CA), at 37°C and 5% CO_2 for 24 h after pancreatic isolation procedures. Islets were collected in conical tubes and centrifuged to proceed with staining. Islets were stained with CellVue™ Maroon Cell Labeling Kit (Thermo Fisher Scientific) according to manufacturer's instructions.

Prior to co-culture with islets, MSC or EC were washed with sterile phosphate buffered saline (PBS; Thermo Fisher Scientific) and detached with TrypLE™ EXPRESS (Gibco, Thermo Fisher Scientific) from culture plastic. Enzymatic reactions were neutralized with corresponding CCM and cell pellets were obtained by centrifugation. EC and MSC were counted and then stained with PKH26 red fluorescent cell linker (Sigma-Aldrich, St. Louis, MO) and CellTracker™ Blue CMAC (Invitrogen), respectively, according to manufacturer's instructions. EC and MSC were re-suspended in complete islet media, counted and proceeded to co-culture conditions.

Using Corning® 96-well Spheroid Microplates (Corning Incorporated, Corning, NY), all four groups of islet constructs were co-cultured prior to modeling transplantation. Approximately, five islet equivalents (IEQ; average 1500 islet cells per cluster) were hand selected and transferred to each wells of all groups. Following, 5.0×10^3 EC and/or 1.0×10^3 MSC were added to appropriate wells to generate Group 2 (islet + EC) constructs (5 IEQ:5.0×10^3 EC), Group 3 (islet + MSC) constructs (5 IEQ:1.0×10^3 MSC) and Group 4 (islet + EC + MSC) constructs (5 IEQ:5.0×10^3 EC:1.0×10^3 MSC). All conditions were maintained in culture and self-assembled into spheroids at 37°C and 5% CO_2 for 48 h.

Vascular bed assembly as transplantation site

Cultrex PathClear Reduced Growth Factor Basement Membrane Extract (R&D Systems, Inc., Minneapolis, MD) was thawed overnight at 4°C, and 80 µl was added to each well of a Corning™ Falcon™ 96-well Imaging Microplate (Thermo Fisher Scientific). Plates were subsequently centrifuged at 3000 rpm for 10 min at 4°C and transferred to incubators set at 37°C for at least 30 min for gelation before the addition of cells. Simultaneously, EC were collected as previously described and stained with PKH67 green fluorescent cell linker (Sigma-Aldrich) according to manufacturer's instructions. EC were re-suspended in complete EGM-2 at 1.5×10^5/ml, and 100 µl of cells were seeded into each basement membrane extract-coated well. Plates were transferred to incubators set at 37°C and 5% CO_2 and self-assembly of vascular beds was achieved within 24 h.

Transfer and maintenance of islet constructs for Model-Tx

According to the schematic in Figure 1, islet constructs for all four groups were individually transferred to a well containing the vascular beds using a micropipette. Constructs randomly distributed and localized to the vascular beds. One hundred microliter (100 µl) of complete islet media was added to the remaining complete EGM-2 media, and microplate was transferred to an incubator set at 37°C and 5% CO_2. After 24 h, media from each well was collected and stored at −20°C for further analysis, and fresh complete islet media was replaced every 24 h prior to imaging.

Microscopic imaging and quantitative analysis of neo-vascularization

Bright field and fluorescence images of all constructs before and after Model-Tx were acquired using an Eclipse Ti2 microscope (Nikon Instruments, Inc., Melville, NY). Additionally, Z-stack confocal images were captured at 72 h after Model-Tx for 3D rendered images using a Leica TCS SP5 confocal microscope (Leica Microsystems Inc., Buffalo Grove, IL), which were imported into SyGlass software (IstoVisio, Inc., Morgantown, WV) for virtual reality generated videos.

Images (2-D) of constructs taken at 10× magnification were further analyzed every 24 h for measurement of construct sizes and parameters of neo-vascularization upon Model-Tx. Images were first uploaded into ImageJ software (National Institute of Health, Bethesda, MD). Diameters of each construct were measured in ImageJ for all groups ($n = 8$). To quantitatively compare neo-vascularization, fluorescein isothiocynate (FITC) channel images were uploaded into ImageJ software and converted to binary using Otsu thresholding. This method was experimentally tested against other thresholding methods in order to find a consistent and objective means of normalizing the intensities of all images. Particles were then analyzed for surface area measurements positive for vb-EC surrounding each construct. For branching, FITC channel images were used to count the number of branches radiating directly to the construct. Analysis was performed on images from all groups ($n = 5$) from 24–72 h after Model-Tx.

Enzyme-linked immunosorbent assays

Conditioned media obtained from co-cultures were thawed, and protease inhibitor cocktail was added to stabilize proteins. Each sample was diluted (1:50) with distilled water. Human C-Series enzyme-linked immunosorbent assays (ELISA) growth factor arrays (RayBiotech Life, Inc., Norcross, GA) were performed with samples from each group ($n = 5$) according to manufacturer's instructions.

Glucose-stimulated insulin secretion

GSIS assays were performed to assess functionality of islet constructs after 72 h after Model-Tx. Constructs were first equilibrated for 1 h in buffer solution (125 mM NaCl, 5.9 mM KCl, 2.56 mM $CaCl_2$, 1.2 mM MgCl, 25 mM HEPES and 0.1% w/v bovine serum albumin; pH 7.4) containing low glucose (2.8 mM). Then, constructs were sequentially incubated at 37°C in fresh low glucose buffer solution followed by high glucose (16.8 mM) buffer solution for 40 min interspersed by a wash with PBS. After incubation in low or high glucose solutions, the supernatant from each sample ($n = 11$ per group) was collected and insulin concentration was detected using an ELISA kit for human insulin (10-1113-10; Lot #29177, Mercodia, Sweden) according to the manufacturer's instructions. Concentrations were calculated by a plate reader (Beckman Coulter DTX880 Multimode Detector)

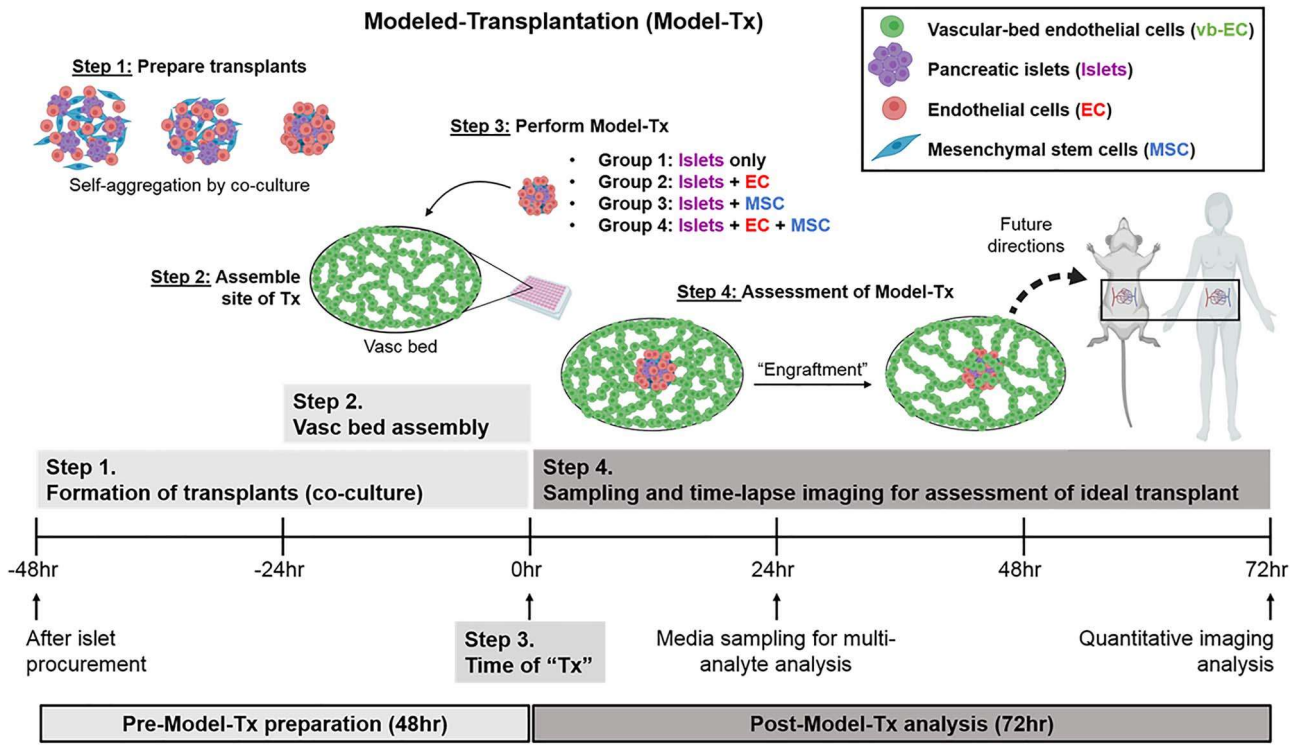

Figure 1. Schematic of pancreatic islet transplantation using *in vitro* model. Co-transplantation strategies for improving islet neo-vascularization were explored using a controlled and simplified *in vitro* method. Step 1: Several fluorescent stains were employed for each cell type and co-cultured according to designated group for 48 hours. Step 2: Vascular (vasc) beds were assembled as model transplantation (Tx) sites. Step 3: Time of Tx was designated as the event when a construct from each group ($n = 8$) was transferred, or "transplanted", onto a vasc bed. Step 4: Acquisition of images for qualitatively and quantitatively analyses after experimental islet constructs were transplanted, or Post-Model-Tx. Images created with BioRender.com. Abbreviations: endothelial cells (EC), mesenchymal stem cells (MSC), vascular bed EC (vb-EC).

with Multimode Analysis Software v3.3.0.9 using a cubic spline regression of the absorbance at 450 nm of standards minus absorbance of the blank.

Statistical analysis

Quantitative comparisons were performed using one-way or two-way ANOVA followed by Bonferroni or Dunnett multiple comparisons test, respectively, using Prism v8 software (GraphPad, San Diego, CA). All values were represented as the mean ± standard error of the mean, and statistical significance was reported against the islet-only group for comparison (*, $P < 0.05$; **, $P < 0.01$; ***; $P < 0.001$).

RESULTS

Assembly of *in vitro* transplantation model is rapid and reproducible

Islet-only or heterotopic islet constructs were strategically generated with or without the additions of EC and MSC according to designated group. Preliminary optimization indicated that the combination of islets, EC and MSC required 24–48 h of self-aggregation into a spheroid that was then able to recruit the vb-EC at a controlled rate during Model-Tx. Reduced aggregation times resulted in complete dissociation of vascular networks, disassembly of islet constructs and/or total (i.e. uncontrolled) recruitment of vb-EC to islets constructs (Supplementary Fig. S1). Therefore, islet constructs were consistently and reproducibly generated by allowing co-culture times of 48 h for each group. Although islets are irregular clusters of cells, the addition of EC and more noticeably MSC assembles a more uniformly shaped single spheroid construct after 48 h (Fig. 2A). Time-lapse imaging using fluorescence microscopy captured the progression of tube formations, and complete vascular beds of assembled vb-EC were achieved by 24 h of seeding. By standardizing protocols for the 24-h duration, complete vascular beds were easily achieved and reproducible, which can be verified at low and high magnifications using either bright field or fluorescence filters (Fig. 2B).

Markedly enhanced recruitment of vb-EC to Group 4 (islets + EC + MSC) constructs

Recruitment of vb-EC towards and subsequently into each construct was visualized and quantified to determine, which cellular composition mediated the greatest or ideal pro-angiogenic and pro-vasculogenic signaling. Fluorescence staining of these cells captured the changes to the vascular beds relative to the transplanted constructs over 72 h (Fig. 3). Neo-vascularization was quantified by total surface area of $FITC^+$ vb-EC localized to the area of interest containing the constructs. Within 24 h, neo-vascularization was significantly greater with the Group 4 constructs ($4.88 \times 10^4 \pm 4.68 \times 10^3$ μm^2; $P < 0.01$) compared to Group 1 (islets alone; $2.16 \times 10^4 \pm 1.30 \times 10^3$ μm^2), suggesting most rapid recruitment than all other groups. Both Group 2 (islets + EC; $3.08 \times 10^4 \pm 7.39 \times 10^3$ μm^2) and Group 3 (islets + MSC; $4.08 \times 10^4 \pm 5.74 \times 10^3$ μm^2) constructs enhanced recruitment within 24 h of Model-Tx more than the islets alone.

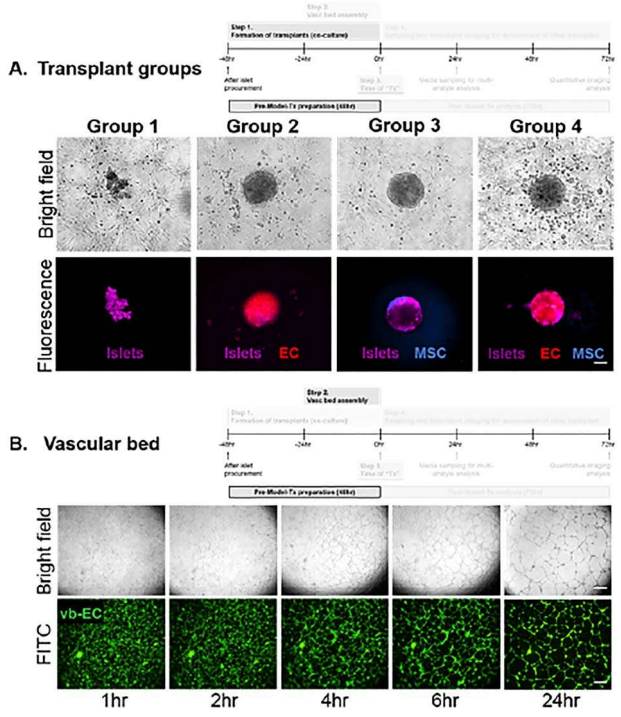

Figure 2. Assembly of islet construct groups and vascular beds prior to Model-Tx. A. All cell types were stained and designated to groups and co-cultured for 48 hours for the formation of constructs. Scale bar represents 100 µm. B. Microscopic images captured at 10× magnification show time-lapse self-assembly of vb-EC into networks that represent the sites of transplantation. Scale bars indicate 500 µm. Group 1: Islets only, Group 2: Islets+EC, Group 3: Islets+MSC, Group 4: Islets+MSC+EC. Abbreviations: Modeled transplantation (Model-Tx), endothelial cells (EC), mesenchymal stem cells (MSC), vascular bed EC (vb-EC).

By 48 h, neo-vascularization was comparable between all groups. Although there were no significant differences, Group 4 (islet + EC + MSC) constructs ($1.66 \times 10^5 \pm 4.68 \times 10^3$ µm^2) achieved the largest increase in neo-vascularization, followed by Group 1 (islets alone; $1.39 \times 10^5 \pm 2.13 \times 10^4$ µm^2), Group 3 (islets + MSC; $1.12 \times 10^5 \pm 3.74 \times 10^3$ µm^2), and Group 2 (islets + EC; $8.01 \times 10^4 \pm 1.01 \times 10^3$ µm^4) at 72 h of Model-Tx (Fig. 4A).

Vascular branches comprised of the FITC$^+$ vb-EC (green) intersected with all constructs within 24 h of Model-Tx, which subsequently increased every 24 h thereafter indicated by enhanced FITC$^+$ cells localized at the construct transplantation sites. Images clearly show the Group 4 and Group 3 constructs (islets + MSC and ± EC, respectively) with significantly greater numbers of vascular branching at all time points compared to Group 1 (islets alone). At 24, 48 and 72 h of Model-Tx, Group 4 constructs were associated with averages of 6.2 ± 0.5 ($P < 0.001$), 6.2 ± 0.5 ($P < 0.001$), and 6.4 ± 0.4 ($P < 0.05$) branches, respectively. Group 3 (islet + MSC) constructs also had significantly more branching at 24 h (5.8 ± 0.5; $P < 0.01$), 48 h (5.6 ± 0.5; $P < 0.01$) and 72 h (6.6 ± 0.4; $P < 0.05$) compared to Group1 (islets alone) with 3.6 ± 0.2, 3.4 ± 0.5 and 4.8 ± 0.6 branches at 24, 48 and 72 h, respectively. Displaying an opposite trend, the total branches to Group 2 (islets + EC) constructs decreased from 4.4 ± 0.8 branches at 24 h to 3.6 ± 0.2 and 3.8 ± 0.6 branches at 48 and 72 h after Model-Tx, respectively.

Increasing sizes of the constructs is another assessment of neo-vascularization as vb-EC integrate into the constructs to establish cellular connections. At 24 h post-Model-Tx, Group 3 (islets + MSC) constructs (261 ± 6 µm; $P < 0.05$) exhibited the largest construct diameter followed closely by the Group 4 constructs (islets + EC + MSC; 242 ± 10 µm) whereas Group 2 constructs (islets + EC; 213 ± 28 µm) and Group 1 (islets alone; 182 ± 30 µm) were smaller in size. At 48 h, Group 4 constructs (islets + EC + MSC; 273 ± 22 µm; $P < 0.05$) and Group 3 constructs (islets + MSC; 271 ± 13 µm; $P < 0.05$) were markedly larger in size than Group 1 (islets alone; 200 ± 19 µm). A slight increase in size was seen in Group 1 (islets alone; 206 ± 10 µm) by 72 h post-Model-Tx, while Group 4 constructs (islets + EC + MSC; 310 ± 26 µm; $P < 0.001$) and Group 3 constructs (islets + MSC; 290 ± 7 µm; $P < 0.01$) were significantly larger in size suggesting robust recruitment and neo-vascularization from the surrounding vascular bed. Consistent with previous neo-vascularization parameters from the Group 2 (islets + EC) constructs, construct sizes decreased from 237 ± 24 µm to 195 ± 13 µm at 48 and 72 h post-Model-Tx, respectively (Fig. 4C). For a more detailed visualization of this analysis, see Figure 5.

In support of the above data, qualitative evidence was obtained from representative images rendered in 3D and virtual reality videos. These depictions not only demonstrate the co-localization of the vb-EC to Group 4 (islets + EC + MSC) constructs but also the integration within the constructs. Furthermore, this imaging shows the intravascular networks achieved by the cells composing the Group 4 constructs (islets + EC + MSC; Supplementary Movie S1). Together, these compelling imaging strategies bolster the quantitative analysis techniques of vb-EC analysis to assess neo-vascularization.

Functional assessments showed lower insulin secretion in constructs containing MSC

Islet function of each construct was quantitatively compared by low and high glucose challenges and subsequent detection of secreted insulin. Significant differences in secreted insulin were measured for the low (905.66 ± 93.28 mU/L) and high (1738.88 ± 446.17 mU/L; $P < 0.0001$) glucose challenges in Group 1 (islet only). Similar secreted insulin levels were measured in Group 2 (islets + EC) for the low (989.44 ± 259.99 mU/L) and high (1826.88 ± 524.32; $P < 0.0001$ mU/L) glucose challenges. Although Group 3 (islets + MSC) maintained comparable secreted insulin levels in the low glucose challenge (932.32 ± 260.98 mU/L), the high glucose challenge (1498.50 ± 349.49 mU/L; $P < 0.01$) showed a reduction in secreted insulin. Secreted insulin measured during the low glucose challenge (978.06 ± 340.11 mU/L) in Group 4 (islets + MSC + EC) was comparable to the levels in all groups; however, levels of secreted insulin during the high glucose challenge (1291.10 ± 210.20 mU/L) was substantially decreased (Fig. 4D).

Group 4 (islets + EC + MSC) constructs show modulated secretory profiles

Growth factor ELISA detected several proteins with angiogenic activities; however, among those detected were basic fibroblast growth factor (FGF), endothelial growth factor (EGF), IGF-1 and vascular endothelial growth factor (VEGF); all of these were exogenous supplements to the media that the vb-EC cultures for vascular bed formation during initial assembly. Although media was removed and replaced with islet media for the remainder of the Model-Tx period, these proteins were removed from the analyses to avoid confounding effects of any potential residues. Discerning the profiles of growth factors with multi-cellular constructs relies on comparing each group to all other groups. Between Group 1 (islets only) and Group 2 (islets + EC groups),

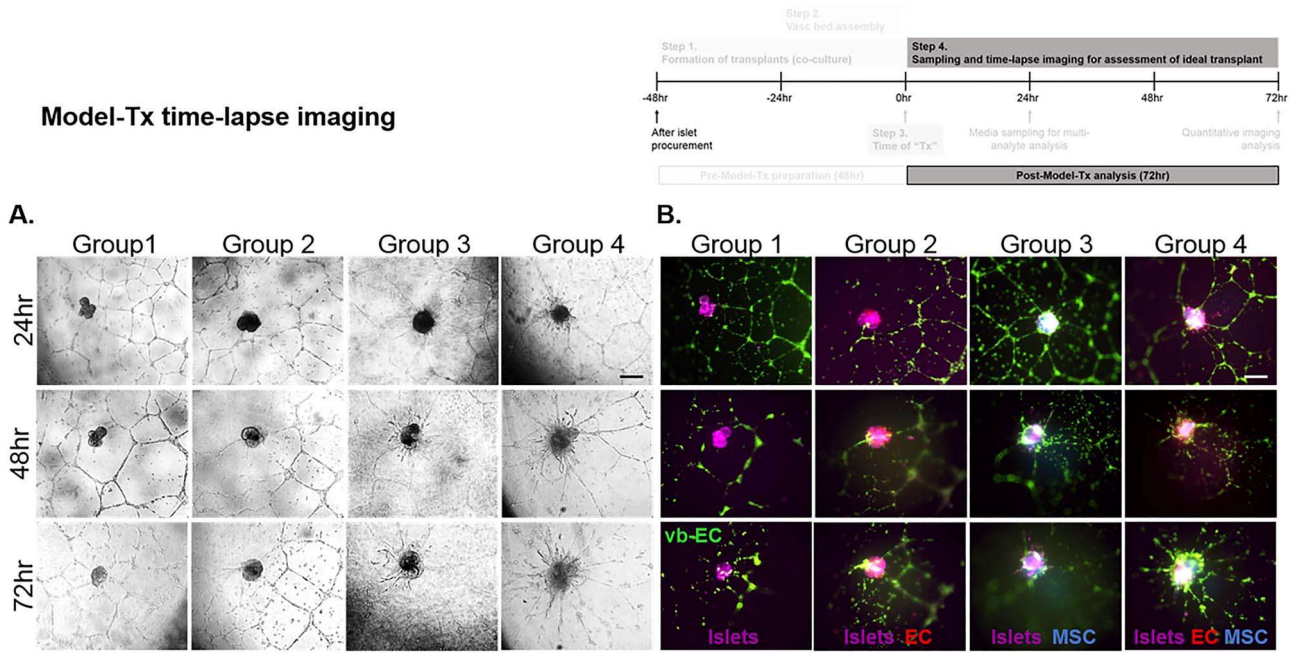

Figure 3. Time-lapse imaging of islet groups during modeled transplantation (Model-Tx). Bright field (A) and fluorescence (B) images taken at 10× magnification show representative constructs for each group at 24, 48, and 72 hours after Model-Tx. Time-lapse images illustrate the cellular orientation of cells composing the islet constructs and their temporal and spatial relationships with the vascular bed. Scale bars represent 200 µm. Group 1: Islets only, Group 2: Islets+EC, Group 3: Islets+MSC, Group 4: Islets+MSC+EC. Abbreviations: Modeled transplantation (Model-Tx), endothelial cells (EC), mesenchymal stem cells (MSC), vascular bed EC (vb-EC).

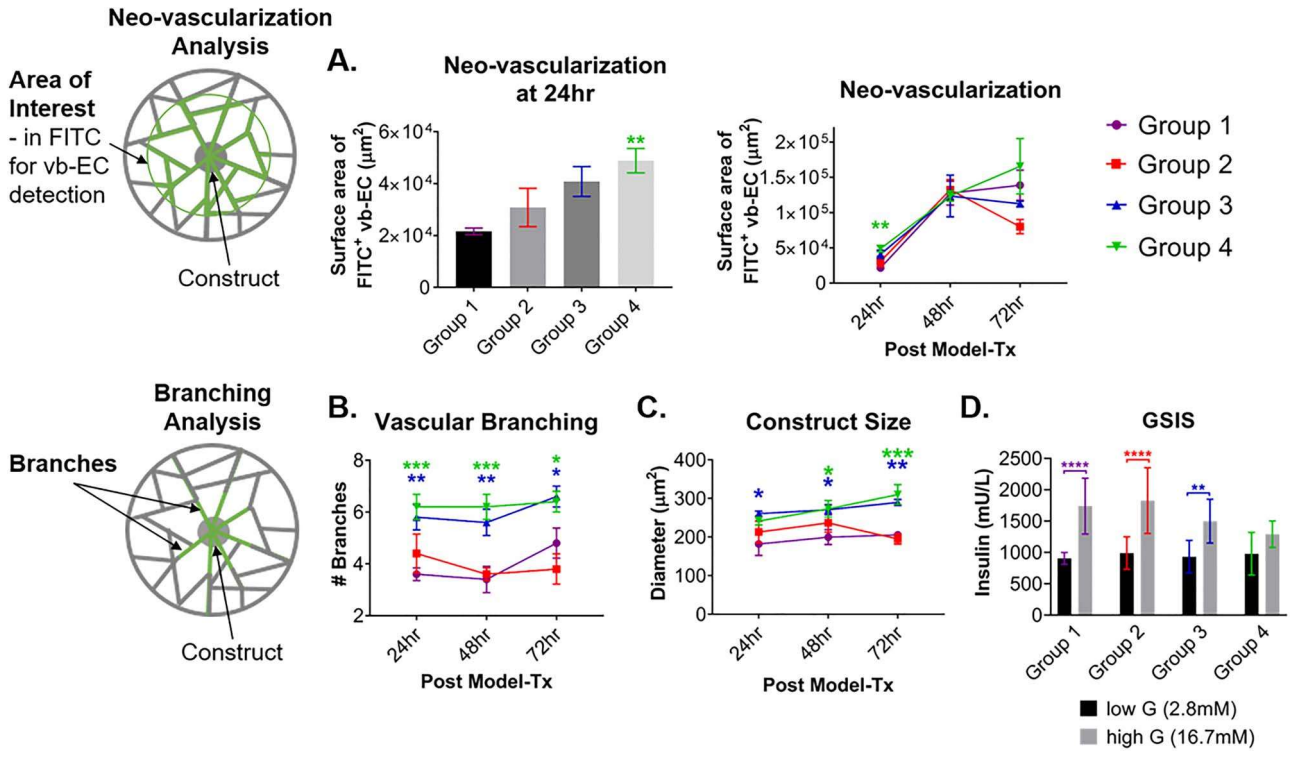

Figure 4. Vascular bed remodeling analyses and islet function. Fluorescence staining enabled detection of FITC^{+} vb-EC when recruited into the area of interest surrounding the constructs during the 72hr of Model-Tx. A. Recruitment and co-localization of vb-EC from vasc bed was quantitatively compared between all groups to suggest rapid recruitment, as demonstrated by the 24hr time point, and degree of engraftment throughout the 72hr period. B. Vascular branching was determined by the number of radial striations to islet constructs created by vb-EC. C. Diameters of each islet construct was measured to demonstrate changes in size subsequent to vb-EC recruitment. D. Low and high glucose challenges demonstrated islet function measured as insulin secretion. *, $p<0.05$; **, $p<0.01$; **, $p<0.001$ compared to islet only group. Color denotes islet group comparison. Group 1: Islets only (purple), Group 2: Islets+EC (red), Group 3: Islets+MSC (blue), Group 4: Islets+MSC+EC (green). Abbreviations: Modeled transplantation (Model-Tx), endothelial cells (EC), mesenchymal stem cells (MSC), vascular bed EC (vb-EC), Glucose stimulated islet secretion (GSIS).

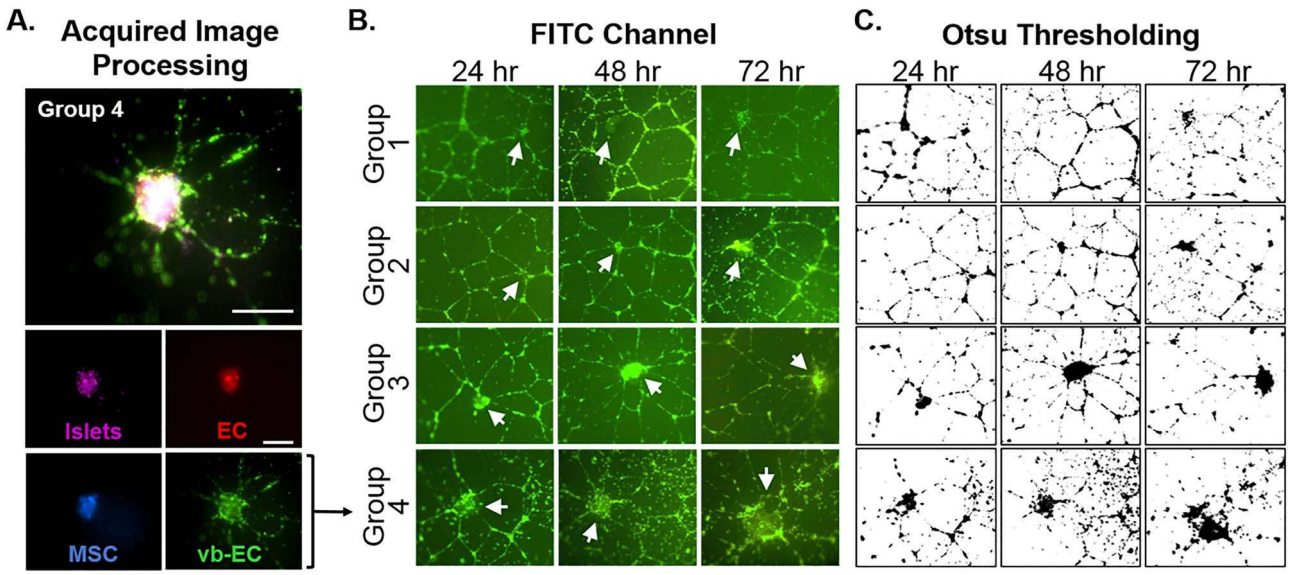

Figure 5. Image acquisition and processing for quantitative analysis of neo-vascularization. A. Fluorescence image of a vascularized islet at 72hr post Model-Tx demonstrates the separation of fluorescence channels to distinguish each cell type enabled imaging, standardization, and subsequent quantification of parameters of neo-vascularization (i.e., recruitment of vb-EC, vascular branches, and construct size). Scale bar indicate B. FITC channel images were collected for each group ($n = 5$) and further processed. High intensity images show the concentration of $FITC^+$ vb-EC localized around islet constructs (white arrows). After FITC channel images were imported into ImageJ, Otsu thresholding was used to standardize parameters of detection for each image which was then converted to a binary image for quantitative analysis. Group 1: Islets only, Group 2: Islets+EC, Group 3: Islets+MSC, Group 4: Islets+MSC+EC. Abbreviations: Modeled transplantation (Model-Tx), endothelial cells (EC), mesenchymal stem cells (MSC), vascular bed EC (vb-EC).

the secretory profile of the additional EC contribution to the constructs showed a large presence of common EC mediators including amphiregulin, heparin-binding EGF, IGF binding protein (IGFBP) proteins, and platelet-derived growth factor proteins (Fig. 6A).

Interestingly, the profiles of growth factors secreted by the constructs containing MSC, i.e. Group 4 (islets + EC + MSC) and Group 3 (islets + MSC) constructs, demonstrated an overall reduction in detected proteins present in the conditioned media compared to Group 1 (islets alone) and Group 2 (islets + EC) constructs. The most significantly attenuated secretory proteins, compared to the Group 1 (islet alone) were granulocyte-colony stimulating factor (G-CSF; 0.40 ± 0.07-fold; $P < 0.05$) and IGF-2 (0.29 ± 0.07-fold; $P < 0.05$), which were measured from the Group 4 constructs (islets + EC + MSC). The growth factors of the IGFBP family were most modulated among the groups. More specifically, Group 4 (islets + EC + MSC) and Group 2 (islets + EC) constructs secreted increased levels of EGF receptor, IGFBP-3, IGFBP-4, and most notably from the Group 4 constructs (islets + EC + MSC), IGFBP-6 (Fig. 6B). Group 4 (islets + EC + MSC) constructs also demonstrated relatively higher levels of FGF proteins including FGF-4, FGF-6 and FGF-7 (Fig. 6A).

3D rendered images reveal visible neo-vascularization into constructs containing MSC

Confocal imaging acquired Z-stack images taken of representative constructs for each group after 72 h post-Model-Tx. By selecting and imaging individual fluorescence channels, multiple perspectives were generated to portray the localization of the constructs relative to the vb-EC. Most importantly, 3D planar views show the side angle of the $FITC^+$ vascular bed, highlighted by the white dotted line, revealing the protrusion of vb-EC that surround and have integrated directly into the constructs, occurring only in Group 4 (islets + EC + MSC) and Group 3 (islets + MSC) constructs (Fig. 7). Videos of 3D generated constructs show the representative constructs for better visibility of cellular orientations after 72 h of Model-Tx (Supplementary Movie S1).

DISCUSSION

Vast evidence from *in vivo* studies has compiled a strong foundation for translational research, yet predictive outcomes are confounded by the complexity of multiple organ systems working in tandem making simplified *in vitro* models and organ-on-chip platforms attractive for many applications [14–16]. Growing interest has focused on reducing these complex networks of activities to *in vitro* platforms that model specific cellular interactions in order to identify and better understand translational mechanisms and their corresponding contributions. Pioneers for organ-on-chip developments have substantiated a vital need for narrowing the complexities of organ systems to investigate and carefully tune pertinent aspects of physiological mechanisms with reproducible outcomes [14, 16]. These *in vitro* platforms have the potential to not only model diseases, personalize therapies, and evaluate high-throughput testing of pharmaceuticals, but also to allow access into key systems that are not permitted by *in vivo* models [15, 17, 18].

Here, we demonstrate a platform that models transplantation to parallel and corroborate an *in vivo* study by Takahashi *et al.* [10]. The success of pancreatic islet transplantation is contingent on several factors, from the rigorous islet procurement procedures from healthy donor pancreases to the engraftment into T1D recipients [19, 20]. Furthermore, immune system reactivity for allografts and potential re-emergence of autoreactivity against transplanted cells after engraftment are a few of the many areas pursued by preclinical and clinical investigations to improve this process [9, 21]. MSC have demonstrated safety in several clinical trials when combined with solid organ transplantation and cell therapy, yielding strong

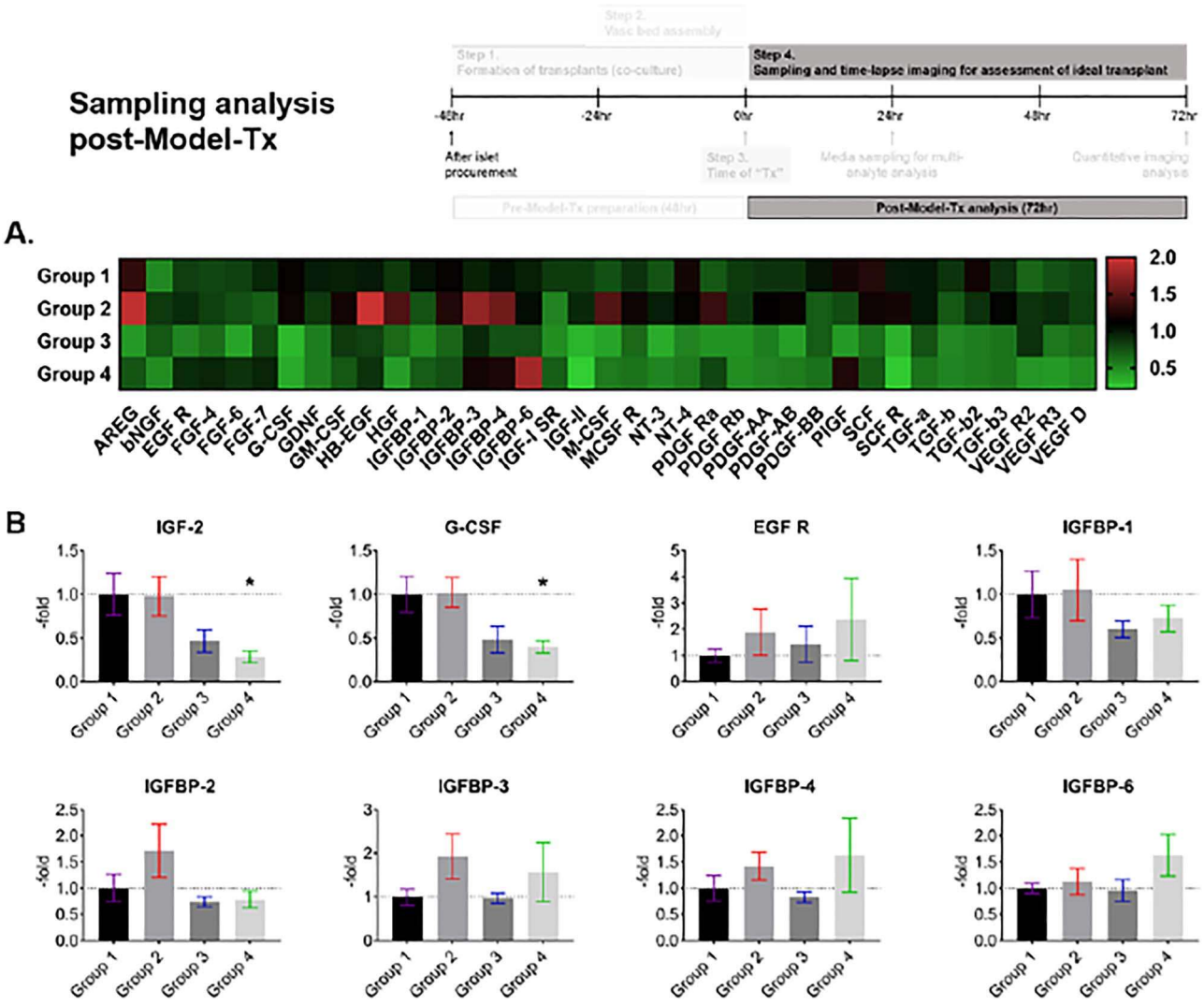

Figure 6. Growth factor profiles determined mediators of neo-vascularization. A. Heat map representation of enzyme-linked immunosorbent assay results of human growth factors that were secreted into the media and sampled from the first 24 hours after Model-Tx. B. Proteins of the vascular endothelial growth factor and insulin-like growth factor families known to mediate pro-angiogenic and pro-vasculogenic processes. Quantitative comparisons were made normalized to Islets only (=1) and revealed large differences between each group ($n = 5$) correlative to their composite cellular contributions. *, $p<0.05$ compared to Islets only. Group 1: Islets only, Group 2: Islets+GroupEC, Group 3: Islets+MSC, Group 4: Islets+MSC+EC. Abbreviations: Modeled transplantation (Model-Tx), endothelial cells (EC), mesenchymal stem cells (MSC), vascular bed EC (vb-EC).

evidence for their capabilities as therapeutic modalities [22–24]. MSC are maintained in the perivascular niche and inherently relay molecular signals with the vasculature through a tight interaction with EC [25, 26]. Mediating angiogenic signaling as well as modulating immune system responses and inflammation is the more well-investigated therapeutic effects of MSC [25, 27, 28]. Islets are clusters of endocrine cells that function in response to molecules in the blood. Proximity to the bloodstream and high oxygen demands are requisite for islet survival and function, thus are of high importance after islet transplantation. These priorities have led to experimental strategies to optimize the site of transplantation such as portal vein infusion and omental transplantation. However, strategies for enhancing neo-vascularization potential and transplantation sites of the islets remain of great interest [29–32]. An alternative approach for improving neo-vascularization of transplanted islets has been evaluated by initiating pre-vascularization strategies prior to transplantation. Using co-culture techniques, MSC and EC have been combined with islets to generate constructs called vascularized islets. Short-term co-culture (48 h) has demonstrated initiation of intravascular networks that have been suggested to improve neo-vascularization once transplanted *in vivo* [10]. However, investigating the mechanistic underpinnings and contributions of each cell type during neo-vascularization after transplantation is limited using animal models. By modeling transplantation *in vitro*, imaging, sampling, and simplification from coordinated organ systems permit access into mechanisms of interest to directly study the controlled outcomes of specific therapeutic strategies. In this study, an *in vitro* vascular bed simulating a transplantation site was used to demonstrate a controlled method to quantitatively compare the angiogenic and vasculogenic properties of heterotopic islets, to reproduce and validate previously reported *in vivo* evidence.

During the 48-h co-culture, Group 4 (islets + EC + MSC) and Group 3 (islet + MSC) constructs were rapidly assembled

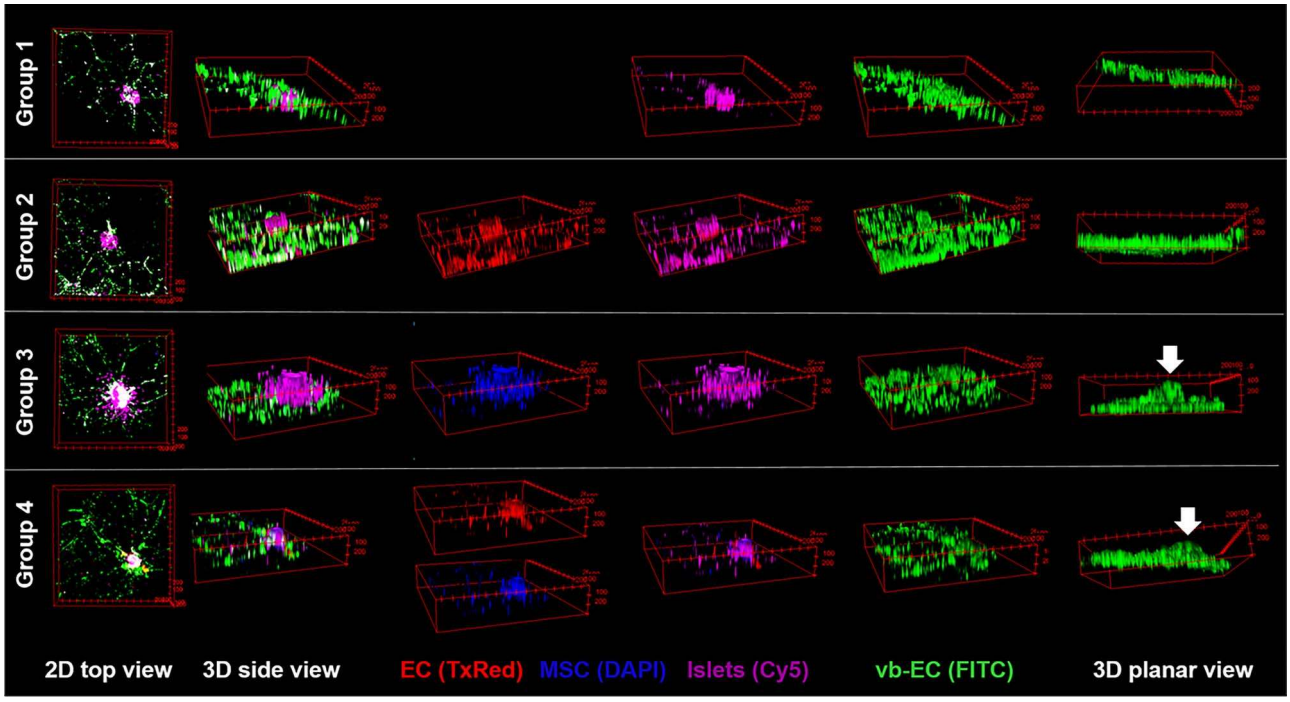

Figure 7. 3D images of islet groups after Model-Tx. Confocal images were acquired as Z-stacks taken at 10x magnification. Fluorescence channels were separated and organized into several orientations to visualize the composition of the islet construct areas. 3D planar view of $FITC^{+}$ vb-EC shows the level of the vascular bed (white dotted lines) and the protrusion created by vb-EC recruited into the construct visible in Groups 3 and 4 (white arrow). Group 1: Islets only, Group 2: Islets+EC, Group 3: Islets+MSC, Group 4: Islets+MSC+EC. Abbreviations: Modeled transplantation (Model-Tx), endothelial cells (EC), mesenchymal stem cells (MSC), vascular bed EC (vb-EC).

into tightly aggregated spheroids. After Model-Tx, analysis of neo-vascularization, including recruitment, co-localization, and branching of vb-EC, was significantly more rapid and robust with islet constructs containing both MSC and EC, compared to islets alone. Comparatively with the controls, constructs that were co-cultured only with MSC (Group 3) prior to Model-Tx showed similarly rapid and robust effects as the islet constructs containing both MSC and EC (Group 4). This evidence demonstrates the potency of MSC for cell signaling and migration, which is further supported by the reduced parameters of neo-vascularization measured in the Group 2 (islet + EC) control construct that lacks MSC. Furthermore, the pin-wheel-like structures created by vb-EC visualized within the constructs by 72 h suggest intravascular networks. These key features support the proposed mechanisms and results by Takahashi *et al*. [10].

Not only does this model provide a time-lapse view into the coordinated movements that occur after modeling transplantation but also allowed us to directly sample the mediators that guide these processes. Unlike Group 2 (islet + EC) constructs, the secretory profiles of constructs containing MSC show attenuation of common pro-angiogenic signaling. Together with our preliminary evidence, these data suggest that uncontrolled release of mediators can have an untoward effect, which may lead to dissociation of the vasculature bed. MSC inherently receive signals to meet the needs of their surrounding environment, thus a controlled and sustained release of necessary signals may have been the mechanistic action that resulted in rapid and robust neo-vascularization. Many of the active proteins detected in the first 24 h of Model-Tx measured in Group 4 were of the IGFBP family, known angiogenic mediators with coordinating levels to control angiogenesis [33–35]. The largest increase measured by Group 4 (islets + EC + MSC) revealed IGFBP-6 as the highly secreted mediator. IGFBP-6 has known effects to modulate angiogenic signals including controlling the effects of the pro-angiogenic signal IGF-2 [35, 36]. This evidence directly supports the significant reduction of IGF-2 that coincided with increased IGFBP-6 in our system by Group 4 (islets + EC + MSC). Moreover, secretion of G-CSF was significantly downregulated, which has known angiogenic potential and cell mobilization effects. Physiologically, G-CSF is released during inflammation or damage to recruit surrounding EC for local VEGF signaling [37, 38]. This downregulation could suggest a level of control to specifically limit the degree of cell motility that corresponds to the controlled integration of vb-EC while preserving the vascular networks as seen in the time-lapse images.

While *in vitro* platforms will never fully capture the complexities of whole organ systems or organisms, they provide a window into cellular events by sampling and analyses of molecular cues that guide those interactions. Furthermore, they enable functional testing of engineered cellular constructs. By performing GSIS test using sequential low and high glucose challenges, the functional capacity specifically of the islets was determined in each group. Insulin secretion during low glucose challenges in each group was comparable; however, differences among the groups were detectable during the high glucose challenges. Group 1 (islets only) and Group 2 (islets + EC) showed comparable secreted insulin levels in both the low and high glucose challenges, suggesting the addition of EC to the islet constructs did not improve or compromise islet function. Insulin secreted during the high glucose challenge in Group 3 (islet + MSC) and Group 4 (islet + MSC + EC) were reduced suggesting either the functional capacity of islets was compromised by the association with MSC or the competition for glucose altered insulin function in the high glucose system. Group 4 (islets + MSC + EC) showed the largest reduction in insulin secretion during high glucose challenge, and constructs were generated

with the highest number of cells. Thus, it is likely that the competition for nutrients compromised the function of the islets given that MSC are highly glycolytic cells utilizing glucose for energy production [39]. Moreover, our results are consistent with previous reports where *in vitro* assessments of islets co-cultured with MSC showed limited function [40]. Yet, preclinical *in vivo* functional tests with prior co-culture and co-transplantation with MSC showed improvements to islets viability and function [41, 42].

Together, this study demonstrated an *in vitro* technique of Model-Tx that permitted the exploration into investigational cell therapies. By providing a window and sampling capabilities into the rapid processes after 'transplantation', we were able to demonstrate the many parameters that this model produces for analyzing neo-vascularization. In the studies currently underway, the platform is being used to streamline islet transplant protocols, with significant translational implications towards T1D treatment. This model may also be of value to wider fields of research including organoids, induced pluripotent stem cell-derived cell therapeutics and related tissue-engineered products.

CONCLUSION

In vitro models provide valuable tools to represent *in vivo* environments in a simplified and controlled manner to study specific mechanisms of interest. Strategies for cell transplantation for T1D patients were optimized to include heterotopic islet constructs as a potentially improved construct for enhancing neo-vascularization. Our model of transplantation permitted the visualization, sampling and quantitative analysis of islet construct 'neo-vascularization' that can be employed for rapid exploratory investigations for cell transplantation strategies.

SUPPLEMENTARY DATA

Supplementary data are available at *INTBIO Journal* online.

FUNDING

This work was supported by NIDDK-supported Human Islet Research Network (HIRN, RRID: SCR_014393; https://hirnetwork.org; UC4DK104209 to A.A. M.I. is supported by F31DK118860-01A1).

CONFLICT OF INTEREST STATEMENT

None declared.

REFERENCES

1. Atkinson MA, Eisenbarth GS, Michels AW. Type 1 diabetes. *Lancet* 2014;**383**:69–82.
2. Gillespie KM. Type 1 diabetes: pathogenesis and prevention. *CMAJ* 2006;**175**:165–70.
3. Dhaliwal R, Weinstock RS. Management of type 1 diabetes in older adults. *Diabetes Spectr* 2014;**27**:9–20.
4. Mottalib A, Kasetty M, Mar JY et al. Weight management in patients with type 1 diabetes and obesity. *Curr Diab Rep* 2017;**17**:92.
5. Kota SK, Meher LK, Jammula S et al. Aberrant angiogenesis: the gateway to diabetic complications. *Indian J Endocrinol Metab* 2012;**16**:918–30.
6. Bruni A, Gala-Lopez B, Pepper AR et al. Islet cell transplantation for the treatment of type 1 diabetes: recent advances and future challenges. *Diabetes Metab Syndr Obes* 2014;**7**:211–23.
7. Shapiro AM, Ryan EA, Diabetes LJR. Islet cell transplantation. *Lancet* 2001;**358**:S21.
8. Hering BJ, Kandaswamy R, Ansite JD et al. Single-donor, marginal-dose islet transplantation in patients with type 1 diabetes. *JAMA* 2005;**293**:830–5.
9. Berman DM, Willman MA, Han D et al. Mesenchymal stem cells enhance allogeneic islet engraftment in nonhuman primates. *Diabetes* 2010;**59**:2558–68.
10. Takahashi Y, Sekine K, Kin T et al. Self-condensation culture enables vascularization of tissue fragments for efficient therapeutic transplantation. *Cell Rep* 2018;**23**:1620–9.
11. Kang S, Park HS, Jo A et al. Endothelial progenitor cell cotransplantation enhances islet engraftment by rapid revascularization. *Diabetes* 2012;**61**:866–76.
12. Coppens V, Heremans Y, Leuckx G et al. Human blood outgrowth endothelial cells improve islet survival and function when co-transplanted in a mouse model of diabetes. *Diabetologia* 2013;**56**:382–90.
13. Takebe T, Sekine K, Enomura M et al. Vascularized and functional human liver from an iPSC-derived organ bud transplant. *Nature* 2013;**499**:481–4.
14. Huh D, Hamilton GA, Ingber DE. From 3D cell culture to organs-on-chips. *Trends Cell Biol* 2011;**21**:745–54.
15. Huh D, Torisawa YS, Hamilton GA et al. Microengineered physiological biomimicry: organs-on-chips. *Lab Chip* 2012;**12**:2156–64.
16. Ingber DE. Developmentally inspired human 'organs on chips. *Development* 2018;**145**(16).
17. Ingber DE. Reverse engineering human pathophysiology with organs-on-chips. *Cell* 2016;**164**:1105–9.
18. Novak R, Didier M, Calamari E et al. Scalable fabrication of stretchable, dual channel, microfluidic organ chips. *J Vis Exp* 2018. (140), e58151.
19. Ichii H, Ricordi C. Current status of islet cell transplantation. *J Hepatobiliary Pancreat Surg* 2009;**16**:101–12.
20. Nanji SA, Shapiro AMJ. Advances in pancreatic islet transplantation in humans. *Diabetes Obes Metab* 2006;**8**:15–25.
21. Longoni B, Szilagyi E, Quaranta P et al. Mesenchymal stem cells prevent acute rejection and prolong graft function in pancreatic islet transplantation. *Diabetes Technol Ther* 2010;**12**:435–46.
22. Reinders MEJ, van Kooten C, Rabelink TJ et al. Mesenchymal stromal cell therapy for solid organ transplantation. *Transplantation* 2018;**102**:35–43.
23. Franquesa M, Hoogduijn MJ, Reinders ME et al. Mesenchymal stem cells in solid organ transplantation (MiSOT) fourth meeting: lessons learned from first clinical trials. *Transplantation* 2013;**96**:234–8.
24. Cortinovis M, Casiraghi F, Remuzzi G et al. Mesenchymal stromal cells to control donor-specific memory T cells in solid organ transplantation. *Curr Opin Organ Transplant* 2015;**20**:79–85.
25. Caplan AI. All MSCs are pericytes? *Cell Stem Cell* 2008;**3**:229–30.
26. Crisan M, Yap S, Casteilla L et al. A perivascular origin for mesenchymal stem cells in multiple human organs. *Cell Stem Cell* 2008;**3**:301–13.
27. Caplan AI, Correa D. The MSC: an injury drugstore. *Cell Stem Cell* 2011;**9**:11–5.

28. Kehl D, Generali M, Mallone A et al. Proteomic analysis of human mesenchymal stromal cell secretomes: a systematic comparison of the angiogenic potential. *NPJ Regen Med* 2019;**4**:8.
29. Kriz J, Vilk G, Mazzuca DM et al. A novel technique for the transplantation of pancreatic islets within a vascularized device into the greater omentum to achieve insulin independence. *Am J Surg* 2012;**203**:793–7.
30. Kim HI, Yu JE, Park CG et al. Comparison of four pancreatic islet implantation sites. *J Korean Med Sci* 2010;**25**:203–10.
31. Cavallari G, Olivi E, Bianchi F et al. Mesenchymal stem cells and islet cotransplantation in diabetic rats: improved islet graft revascularization and function by human adipose tissue-derived stem cells preconditioned with natural molecules. *Cell Transplant* 2012;**21**: 2771–81.
32. Schmidt C. Pancreatic islets find a new transplant home in the omentum. *Nat Biotechnol* 2017;**35**:8.
33. Granata R, Trovato L, Lupia E et al. Insulin-like growth factor binding protein-3 induces angiogenesis through IGF-I- and SphK1-dependent mechanisms. *J Thromb Haemost* 2007;**5**:835–45.
34. Contois LW, Nugent DP, Caron JM et al. Insulin-like growth factor binding protein-4 differentially inhibits growth factor-induced angiogenesis. *J Biol Chem* 2012;**287**:1779–89.
35. Bach LA. Insulin-like growth factor binding protein-6: the "forgotten" binding protein? *Horm Metab Res* 1999;**31**:226–34.
36. Bach LA. Recent insights into the actions of IGFBP-6. *J Cell Commun Signal* 2015;**9**:189–200.
37. Shojaei F, Wu X, Qu X et al. G-CSF-initiated myeloid cell mobilization and angiogenesis mediate tumor refractoriness to anti-VEGF therapy in mouse models. *Proc Natl Acad Sci USA* 2009;**106**:6742–7.
38. Wengner AM, Pitchford SC, Furze RC et al. The coordinated action of G-CSF and ELR + CXC chemokines in neutrophil mobilization during acute inflammation. *Blood* 2008;**111**:42–9.
39. Nuschke A, Rodrigues M, Wells AW et al. Mesenchymal stem cells/multipotent stromal cells (MSCs) are glycolytic and thus glucose is a limiting factor of in vitro models of MSC starvation. *Stem Cell Res Ther* 2016;**7**:179.
40. Rawal S, Williams SJ, Ramachandran K et al. Integration of mesenchymal stem cells into islet cell spheroids improves long-term viability, but not islet function. *Islets* 2017;**9**: 87–98.
41. de Souza BM, Boucas AP, Oliveira FD et al. Effect of co-culture of mesenchymal stem/stromal cells with pancreatic islets on viability and function outcomes: a systematic review and meta-analysis. *Islets* 2017;**9**:30–42.
42. Montanari E, Meier RPH, Mahou R et al. Multipotent mesenchymal stromal cells enhance insulin secretion from human islets via N-cadherin interaction and prolong function of transplanted encapsulated islets in mice. *Stem Cell Res Ther* 2017;**8**:199.